

# COMPUTATIONAL ANALYSIS OF FDM-PRODUCED COMPONENTS AND IMPORTANCE OF PRINT ORIENTATION

Paul Brayford, Linda Knudsen

## INTRODUCTION

“Additive manufacturing” encompasses a growing range of technologies for producing a wide variety of components, ranging from single-use prototype parts through to end-use components for the aerospace industry. Although additive manufacturing technologies offer a host of benefits, they can also introduce additional difficulties into the computational analyses that many engineers use during the course of a design cycle. For example, performing part manufacture with some additive manufacturing technologies, such as Fused Deposition Modeling™ (FDM), introduces additional variables beyond those found in traditional subtractive manufacturing techniques. In this whitepaper, we examine the nature of material properties in FDM components and the difficulties in applying rigorous analysis. We also construct a demonstrative component to examine the comparative effects of the manufacturing build orientation variable on mechanical response.

## BACKGROUND

Within the engineering sector, additive manufacturing (AM) is of particular interest for a number of reasons. One of the primary driving factors is that it allows developers to design geometry that would otherwise be difficult or impossible to manufacture – creating more optimized shapes with intricate or hollow features, combining multi-part assemblies into a single component, etc. AM can also provide cost savings for components that would traditionally require expensive tooling or machining – whether used for prototyping or low-volume production.

Fused Deposition Modeling™ (FDM) is an AM technology developed in the late 1980s and patented in 1992 [1]. FDM builds three-dimensional objects by using a moveable dispensing head to extrude a thermoformable material into shaped layers. Since the technology's patent expiration in 2009 FDM has seen growth greatly surpassing that of any other AM process, and has been key in bringing the concept of AM into the common lexicon, more commonly referred to as ‘3D Printing.’ The most common materials used with the FDM process, including in the large hobbyist sector, are acrylonitrile butadiene styrene (ABS) and polylactide (PLA). Other polymers are commercially available, including nylon, polycarbonate, and acrylonitrile styrene acrylate (ASA), to name a few [2]. Of the polymers more recently made available for FDM, ULTEM 9085 holds particular interest for engineers given its very favorable mechanical and thermal properties [3] and approval for use in aerospace applications [4], [5].

Although FDM materials like ULTEM 9085 show promise for engineering applications, as we demand more from our designs the components and materials in those designs are often pushed closer to their physical limits. To gain a greater understanding of a design and its limits we can use finite element analysis (FEA) software packages to simulate components with well-defined load cases, allowing close approximation of the resultant stresses, strains, and displacements. The material properties of the component are critical inputs to these analyses. Metal components can generally be treated as linear-elastic isotropic, implying that they have an elastic region with a linear modulus of elasticity, and that the material properties are the same regardless of the direction which is it loaded [6]. In contrast, plastic components have more complicated material properties in that they are generally nonlinear-elastic, where the modulus of elasticity changes as the material experiences strain [7]. Some plastics, as well as most as-printed AM plastics, are even more complicated, behaving in a nonlinear-elastic anisotropic manner. These materials not only see a change in the modulus of elasticity as they experience strain but also exhibit different material properties depending on which direction the material is loaded. Due to their complicated properties, a significant amount of material characterization can be required to enable the analysis of plastic and AM parts.

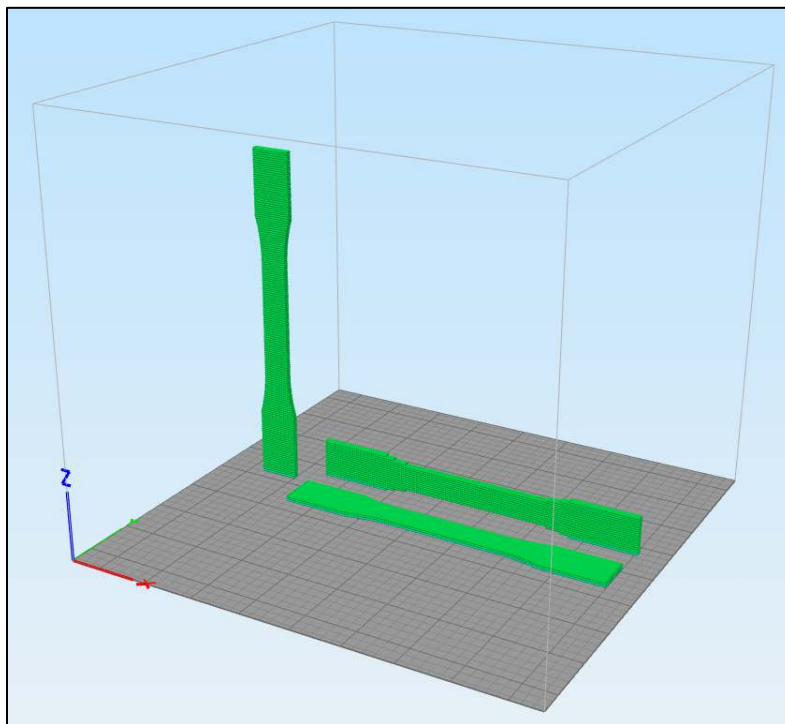
Given the additional material characterization that AM parts demand, it is crucial that the properties are determined in an appropriate manner. Many standard test methodologies provide guidance for the collection of material properties to ensure consistent and appropriate data. Of these, ASTM D638 and ASTM D3039 are both commonly applied standards. ASTM D638 is a “Standard Test Method for Tensile Properties of Plastics,” specifically covering “the determination of the tensile properties of unreinforced and reinforced plastics in the form of standard dumbbell-shaped test specimens” [8]. ASTM D3039 is a “Standard Test Method for Tensile Properties of Polymer Matrix Composite Materials,” determining “the in-plane tensile properties of polymer matrix composite materials reinforced by high-modulus fibers” [9]. Various research has applied one or both of these standards in determining the material properties of as-printed FDM materials. Given the recent approval of ULTEM 9085 for aerospace applications in FDM components, we are specifically interested in the characterization of that material. We have found that much of the current literature on ULTEM 9085 characterization makes use of the D638 standard [10]–[15], including the manufacturer themselves [16], while some choose to apply the D3039 standard [17].

Neither of the D638 or D3039 standards are explicitly appropriate for FDM components. D638 is intended for use with solid injection-molded components, and D3039 is intended for use with plastic/non-plastic composites, both utilizing fabrication techniques far different from the FDM process. There are committees in the process of developing standards specifically around AM parts [18]–[20], but those standards are still in their infancy and not ready for use in characterizing material properties for FDM components.

## **DIFFICULTIES OF FDM ANALYSIS**

### **Anisotropic Nature of FDM**

Much of the research into the material properties of ULTEM 9085 FDM components presents the material as being orthotropic, a subset of anisotropic materials in which the different properties and strengths are in directions perpendicular to each other. This is congruent with the manner in which Stratasys and others interpret ASTM D638 to develop their datasheet for ULTEM 9085, often printing the test samples in three different orientations to capture the properties for each of the Cartesian build orientation possibilities.



*Figure 1: Stratasys Print Orientations for ASTM D638, Layer Thickness Exaggerated. XY (Front), XZ (Rear), ZX (Left).*

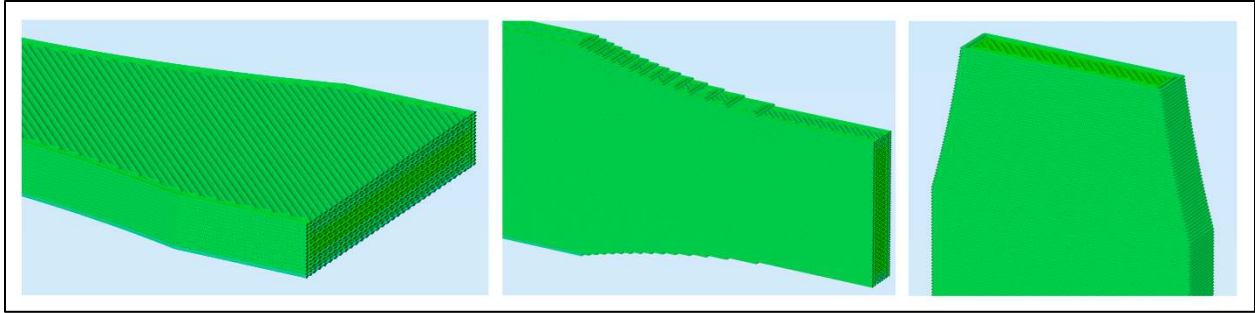


Figure 2: Cross-Section of Each Build Orientation. XY (Left), XZ (Center), ZX (Right).

Figure 1 shows the three printing orientations as defined by Stratasys. The XY sample is layered across the 3.2mm sample thickness, the XZ sample is layered across the 19.0mm sample width, and the ZX sample is layered across the 165mm sample length. Depending on the software used to generate these layers from the solid model, commonly called a 'slicer,' removable material may be added to the print to support the gap under the necked section on the XZ sample, or added to support the high aspect ratio of the ZX sample [10]. Figure 2 shows a cross-section through each of the samples, detailing how the layers are commonly produced. Each layer is comprised of both a 'contour' and an 'infill.' The contour of each layer is a solid loop that circumscribes any outer and inner edges of the layer – in this particular case, each layer has two outer contour loops. The infill is the material that is then rastered to fill the remainder of the layer, commonly produced at 45° or 135° to the contour, alternating between the angles for each layer. Discussion of other layer variables and terminology not discussed here can be found in [21].

Inspection of the theoretical layers within the necked region on the XY and XZ samples shows that the primary difference between the two build orientations is the percentage of infill that comprises the layer, as shown in Figure 3. Assuming a 0.4mm standard nozzle diameter and a dual-loop contour, the XY layer is comprised of 88% infill against the 50% of the XZ sample.

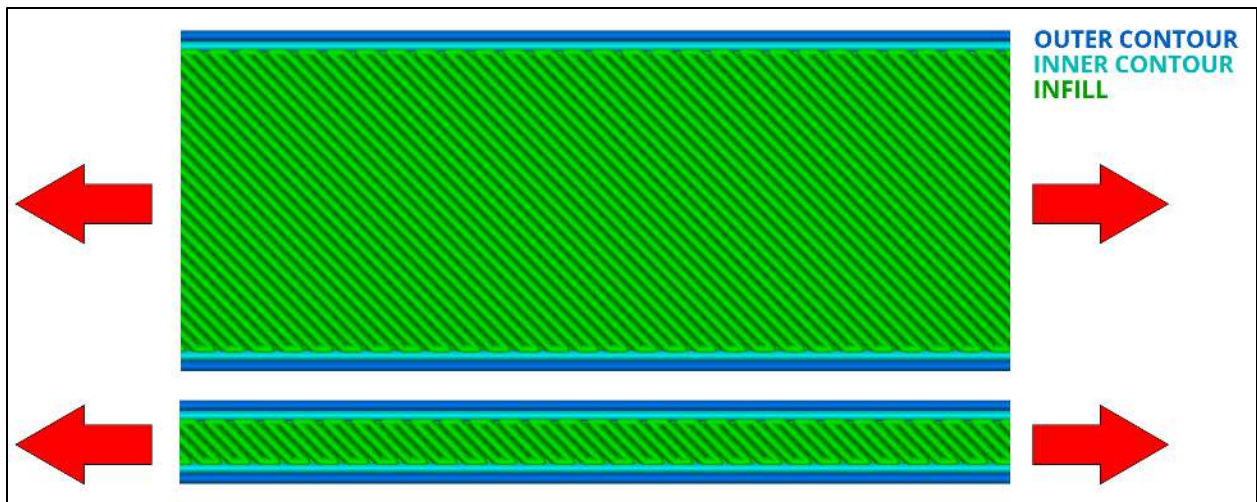
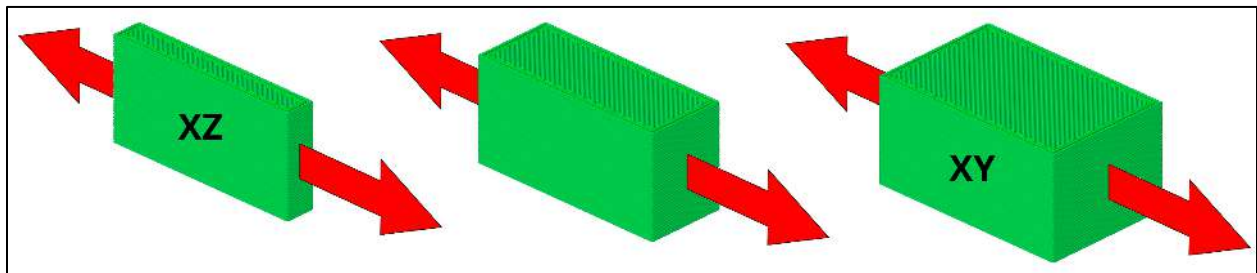


Figure 3: Load Bearing Layer-Cross-Section for XY (Top) and XZ (Bottom)

The difference in build structure between the two build orientations can explain the greater strength that XZ samples exhibit over XY samples [11], [15]. Contour loops on the XY and XZ build orientations align parallel to the pull force when tested per ASTM D638, allowing them to directly resist the tension and rely primarily on the strength of the ULTEM polymer. The infill is at a less advantageous angle to the pull force, relying significantly on

the bond strength between the rastered lines of infill to resist the tension. This bond strength is significantly weaker than the resin itself [22], resulting in an overall lower bulk tensile strength of the infill and a weaker overall cross-section.

Given the observation that infill bond strength plays a significant role in the bulk tensile strength of printed components, we theorize that there is additional material behavior that the direct application of ASTM D638 does not capture. For this discussion, we assume a component with a simple rectangular layer. If we print a rectangular block using rectangular layers that have the same width as the XZ samples, we would expect it to behave with the same properties as the XZ data when loaded in the same tensile direction as the samples. Similarly, we would expect a block printed with layers as wide as the XY samples to follow the response of the XY data. However, given that the percentage of infill is the primary contributor to the variance of as-printed material properties, if we print a rectangular block with rectangular layers that have a width between the XZ and XY samples, we know that the infill percentage will be between 50% and 88% as driven by the block width, and that the material properties of this in-between layer width should fall between the XZ and XY data. All three components are illustrated in Figure 4.



*Figure 4: Rectangular Block Geometry with Varying Properties*

It follows that as the layer width is only defined by component geometry, and can be anything from a single nozzle diameter up to the maximum dimension the printer can produce, there exist differing material property datasets below, in-between, and above, the captured XY and XZ data. We assert that the material data collected from the XY and XZ samples represent only two discrete points along a continuous curve; layer width vs. material performance. This curve describes a material that is geometry-dependent anisotropic, with material properties that vary not only with the direction the load is applied but also with the size of the feature that the load is applied to. Thorough characterization of such a material would be difficult but could theoretically produce a curve for each varying material property against layer width.

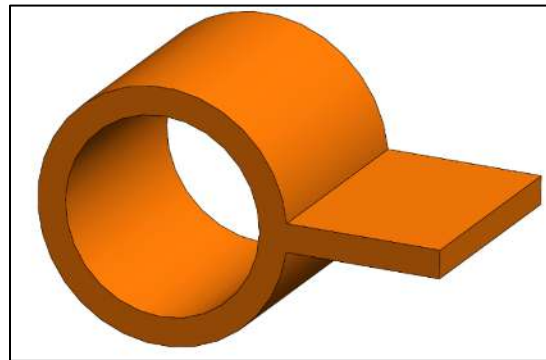
Thermodynamics also enter into the equation for FDM component strength. Layer-to-layer bonding in FDM is dependent on the temperature between the layers of the print. The heat from the new layer being printed will diffuse into the previous layer underneath it, partially re-melting the plastic of the previous layer and developing a bond. The closer the temperatures are between the current and previous layer, the stronger the bond will be [15]. Assuming a constant print speed, it follows that the larger the layers are in total area, the greater the temperature difference will be as the layer being printed over will have had more time to cool. This will in turn develop a weaker layer-to-layer bond. This interaction is nearly impossible to universally characterize given the infinitely variable geometry, layer size, and component layer shape, as well as ambient conditions that could affect the rate at which the lower layers cool.

#### Application of FEA to FDM

Finite element analysis software packages can only provide outputs that are as good as their inputs. FDM components pose a particular challenge when trying to provide high-quality solid model inputs because the solid model that is analyzed may be quite different from the as-printed component that is generated by the slicer. The slicing software has to approximate the solid geometry under the constraints of a defined layer thickness and a fixed extrusion nozzle diameter such that it can be fabricated on the FDM machine. This approximation step

induces voids and an internal structure to the as-printed part that a solid model does not capture [13], [15], [23]. Simulating the FDM build process itself to generate an as-printed part model, then performing an analysis on that as-printed model, could yield a significantly more accurate result. Research has been performed in this direction [22], [24] with promising results, but such an approach is extremely computationally expensive and time-consuming. Commercial packages that can perform analyses on as-printed models are only just becoming available [25] and are not yet widely adopted.

The anisotropic nature of the FDM material is an additional difficulty in providing high-quality inputs to any FEA solver when directly simulating the solid model. It is possible to assign different orthotropic properties to distinct portions of a solid model to account for how the behavior of a single material may differ depending on the geometry [26]. In the referenced example shown in Figure 5, a composite material could be used to fabricate the component, but would result in a portion of the component with a Cartesian anisotropy and a portion with a radial anisotropy.



*Figure 5: Component Example with Multiple Forms of Anisotropy*

Similarly, an FDM component could be designed with a discrete number of wall thicknesses that could be separated into multiple distinct portions and matched with layer widths in geometry-dependent anisotropic data collected for the as-printed material. However, in practice, components are rarely so simple that they can be realistically split into a few distinct portions. In fact, one of the advantages of AM components is that geometry can be significantly more fluid and irregular, lacking any distinct separable portions.

#### Rough FDM FEA Approximation

With rigorous analysis of FDM components requiring either a simple component that is separable into bodies with known distinct anisotropic properties, or a computationally expensive solution methodology, accurate simulation results cannot yet be expected in a current practical engineering environment. Extensive empirical testing on a collection of agreed-upon reference components may allow a set of material properties or other analysis tool inputs to be developed that roughly approximate the behavior of FDM-produced components. Although final component testing would still be required to determine actual behavior and performance, a rough approximation may allow for initial design iteration and reduced non-labor costs. Homogenization theory for periodic media has been studied with success for other types of composite materials [27], which lends credence to the idea that either an analytical or empirical approximation for FDM materials may be possible.

#### EXAMINATION OF PRINT ORIENTATION

Provided the inherent difficulty of rigorous FEA on FDM components and the lack of a set of proven inputs, we turned our focus onto what, as designers, we can easily control (excluding part geometry) that would influence component performance. If we assume that the FDM machine and slicing process is in our control, many FDM process variables can be altered to adjust the print. However, most professional machines already have tuned parameters to produce components to the best of the machine's ability, and are commonly heuristically tuned to achieve the desired result rather than rigorously defined – making further adjustment time consuming and

iterative. Furthermore, given that the equipment capable of producing FDM components from ULTEM 9085 starts around \$185k [28], it is more likely that designers will be working with outside vendors, making it less likely that the designer would have any control over the process parameters.

The one printing variable that a designer can easily specify is the printing orientation. The print orientation determines which side of the part is placed against the print bed, and subsequently which direction the component is layered. Under an assumed set of working loads that the component is expected to experience in use, many components will have an optimal print orientation that provides better overall performance. As presented in [15], changing the print orientation has effects on the modulus of elasticity, strain to failure, and the ultimate tensile strength, for the same ASTM D638 coupon geometry. Similarly, orienting your part such that it is sliced and printed in the most optimal manner can achieve greater performance from the same geometry.

Here we present a constructed example that demonstrates the potential comparative variance among three different print orientations. For this exercise, we make several assumptions in order to demonstrate an analytical difference:

- We assume that the as-printed material is orthotropic, bearing the material properties of the A, C, and D build orientations as defined in [15]. Mapped to the Stratasys nomenclature, the A build orientation matches Stratasys' XY, C matches XZ, and D matches ZX.
- We assume that the material behaves in a linear fashion, and assume a consistent framework on how to apply the XY and XZ material datasets for the layers of each print orientation. The ZX dataset is unambiguous and applied along the layered direction.

With the lack of available and consistent shear or compressive data, we focus exclusively on the tensile performance of the material. Because we do not have empirical data to support or contradict absolute values of the component performance under these assumptions, we examine the analytical outputs on a strictly comparative basis.

### Procedure

The material data presented in [15] provides the ultimate tensile strength, modulus of elasticity, strain to failure, and a combined stress-strain plot for all of the build orientations. As most design engineering is concerned primarily with material yield and not failure, we calculated the 0.2% offset yield strength for the XY, XZ, and ZX build orientations utilizing the provided plot and moduli. While successful for the XY and XZ orientations, the ZX orientation experienced low-strain failure and did not intersect with the 0.2% offset line as shown in Figure 6. The yield-to-ultimate-strength ratio was calculated for the XY and XZ orientations, and used to equivalently derate the ultimate strength of the ZX orientation to obtain the yield strength.



Figure 6: Offset Yield Plot

For our example, we designed a small right-angle mounting bracket, shown in Figure 7, which includes a hollow gusset and three mounting points: two on one flange and the third on the opposite flange. This bracket was designed specifically for FDM manufacture, keeping the walls of the gusset feature to 45 degrees or less from vertical in all intended print orientations to prevent the need for supports during printing [29]. A partially dimensioned drawing including general size and overhang angles is shown in Figure 8.

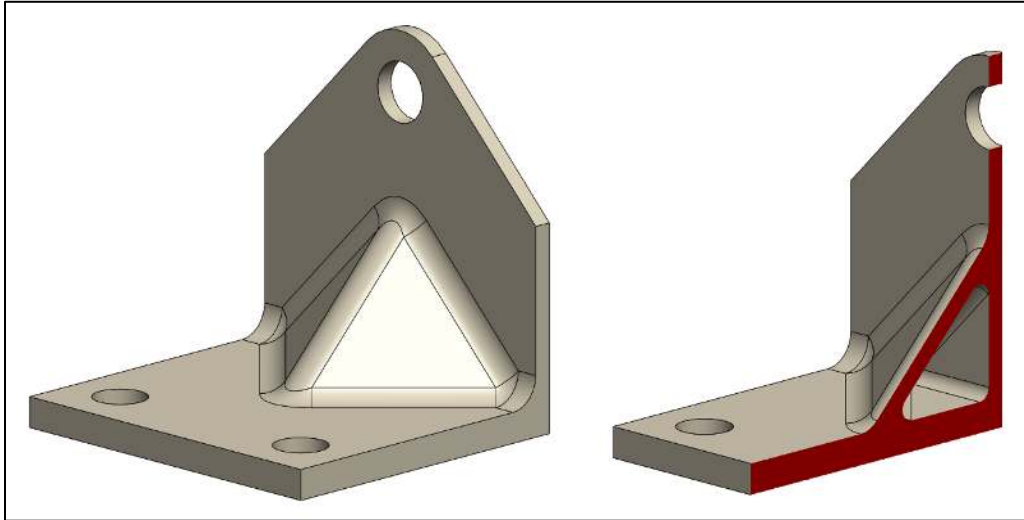


Figure 7: Example Bracket and Cross-Section Showing Hollow Gusset Feature

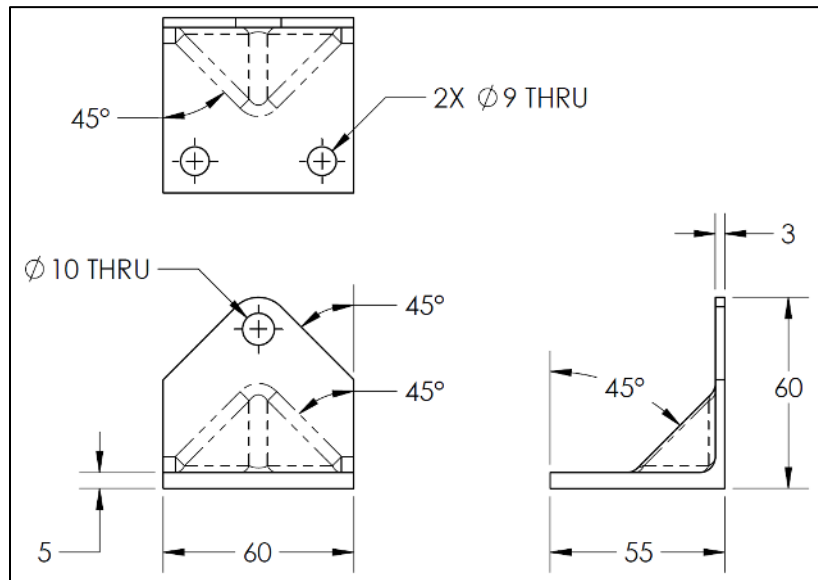


Figure 8: Partially Dimensioned Bracket for Scale, Units in mm

Using both Simplify3D and SolidWorks 2016, we then developed the material properties' framework that defines how the part orientation on the print bed corresponds to the orthogonal directions of the material property. This was done based on the primary print style of the wall that contains the single 10mm diameter hole, the feature to which the loading will be applied. Our first print orientation slices that wall such that, in tension, the wall is best represented by the ZX dataset. Similarly, our second orientation slicing is best represented by the XY dataset, and our third by the XZ. This framework is shown in Table 1.

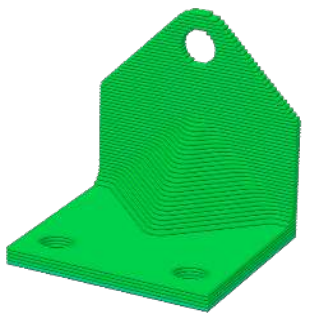
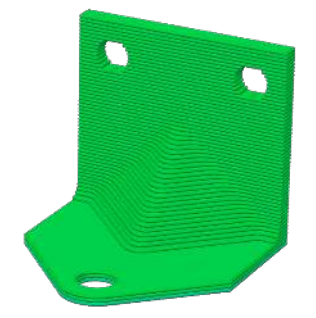
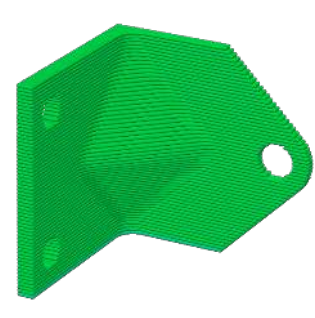
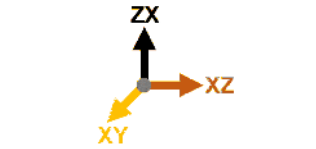
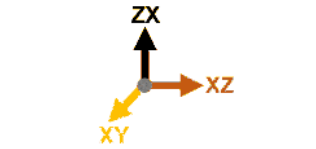
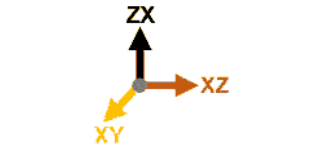
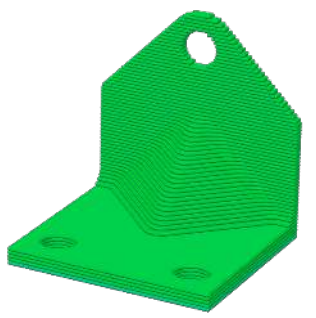

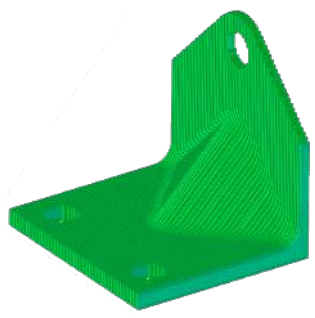
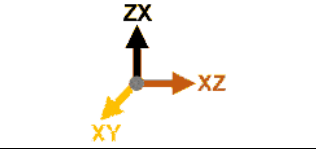
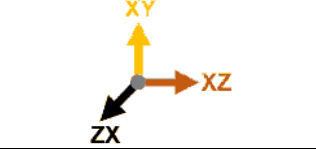
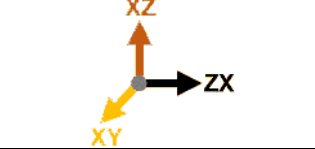
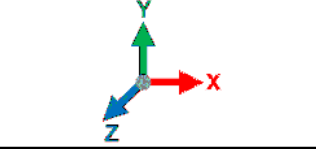
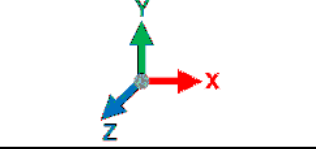
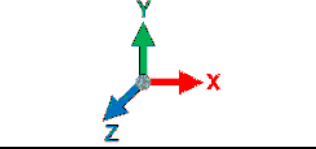
		Orientation		
		1	2	3
Build Orientation				
Build Orthotropy Material Reference Frame				
Loading Orientation				
Loading Orthotropy Material Reference Frame				
Global Coordinate System Solid Model and FEA				

Table 1: Material Property and Build Orientation Framework, Layer Thickness Exaggerated.

With the material framework in place, the simulation was set up to mimic two bolts affixing the lower flange, and a bolt through the 10mm diameter hole in the vertical flange, loaded to 115N in the +Y global direction. Once an appropriate mesh was determined, the simulation was run three times – adjusting only the orientation of the orthotropic material properties in relation to the body to represent the different build orientations.

### Results

For each build orientation simulated, we calculated the tensile factor of safety (FOS) for each orthotropic direction. This was accomplished by projecting the local stress components into the material frame of reference, and dividing the appropriate yield stress by this value. Since the orthotropic frame of reference aligned with the global coordinate system for this setup the projection was handled by the FEA software, which allows the stresses to be calculated normal to any of the Cartesian system directions. The minimum of these FOSs for a given build



orientation was taken as the FOS for the component. We also recorded the maximum vertical displacement for each build orientation. The values used in the calculations and the results are presented in Table 2.

115 N Applied Load	Orientation 1			Orientation 2			Orientation 3		
	XZ	XY	ZX	XZ	XY	ZX	XZ	XY	ZX
<b>Modulus of Elasticity (MPa)</b>	2480	2010	2030	2480	2010	2030	2480	2010	2030
<b>Yield Strength (MPa)</b>	35.3	24.7	19.7	35.3	24.7	19.7	35.3	24.7	19.7
<b>Max. Projected Stress (MPa)</b>	8.2	19.0	21.0	8.9	21.0	19.0	22.2	19.0	6.5
<b>Directional FOS to Yield</b>	4.3	1.3	0.9	4.0	1.2	1.0	1.6	1.3	3.0
<b>Minimum FOS to Yield</b>	0.9			1.0			1.3		
<b>Max. Vertical Deflection (mm)</b>	0.57			0.57			0.54		

Table 2: FOS and Displacement Results

As the stress results are not very visually different between the build orientations, we only present the normal stress projections for the first build orientation in Figure 9.

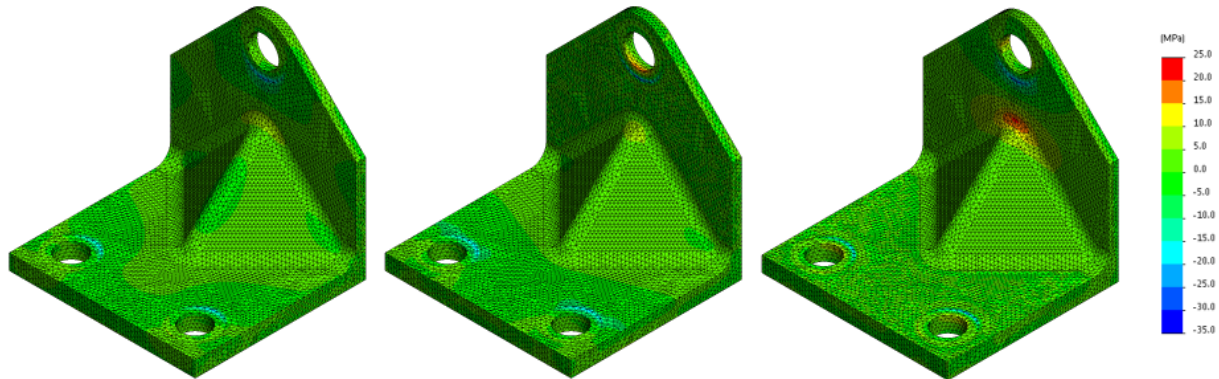


Figure 9: Normal Stress Projections for Orientation 1. XZ (Left), XY (Center), ZX (Right).

### Discussion

While conducted under a set of assumptions that do not explicitly capture the full behavior of the material, the analysis shows that altering the build orientation affects the overall part performance and potentially improves the FOS for a given loading scenario. Using the first orientation as the baseline, the results show an 11% increase in minimum FOS for the second orientation, and a 44% increase for the third orientation. These improvements could be the difference between a part failing under load and surviving with a safety margin left to spare. The component deflection is effectively equivalent between all build orientations, as is expected with the different orthotropic directions bearing similar moduli of elasticity. Other FDM materials may have a larger spread of moduli, in which case this process could also be used to choose the appropriate build orientation to tune part deflection.

This study focused on three build orientations, based on which side of the part was parallel to the print bed. Provided the use of support material to allow high-angle overhangs is acceptable, it is possible to print the part in any orientation within the build volume of an FDM printer. If we assume that one of the flat sides of the component must lie on the print bed, we could rotate the component about the vertical axis and generate a curve relating the angle of rotation to the minimum FOS. The maximum point on this curve would indicate the most advantageous rotation angle at which to print the component, potentially further improving the minimum FOS in loading. Theoretically, this approach could be extended to multiple orientations and curves if there are a few sides of the component particularly suited to be aligned with the print bed, or out to any orientation if the part

does not have any obvious side to place on the print bed. While it might be possible to manually iterate or use an iterative simulation tool such as SolidWorks Optimization for a known set of orientations and rotation axes, more advanced software with robust optimization algorithms would be required to optimally place a component at any orientation in the build volume.

Inspection of the material properties and the potential layering options for a given component design, especially simple components and loading scenarios such as the one presented here, may be sufficient to determine the best orientation for printing, and not require any analysis. More complicated geometry or loading cases may benefit from comparative studies as performed on the bracket example, especially in cases where the expected internal stresses are less obvious. For either approach, these methods only seek to reduce the iterative prototype cycles, not replace them. FDM components must still be empirically tested for performance with a statistically significant sampling set before finalizing a design.

### **SUMMARY**

FDM materials offer a host of benefits for designers but also offer significant challenges when it comes to computationally predicting their behavior. Rigorous material characterization involves a large number of variables and does not yet have any directly applicable testing standard. Furthermore, because material properties of the FDM component can vary across the geometry, accurately creating a representative model in traditional FEA software can be difficult. It is possible to generate accurate models by simulating the print and then running static analysis on that output, but this technique is still in research and only just becoming commercially available.

With rigorous analysis proving to be currently impractical, we examined the comparative impact that the build orientation has on the mechanical response of a constructed component to a tensile loading. Using calculated yield strengths and an assumed orthotropic material framework, we showed up to a 44% difference in minimum FOS simply by adjusting the orientation in which the component is printed, demonstrating the importance of this manufacturing variable.

### **ACKNOWLEDGEMENTS**

We would like to thank Synchroness for making possible the labor of this project, and Dr. John Steuben of the U.S. Naval Research Laboratory for his guidance and technical input.

### **REFERENCES**

- [1] S. S. Crump, "APPARATUS AND METHOD FOR CREATING THREE-DIMENSIONAL OBJECTS," U.S. Patent 5121329A, 1992.
- [2] "FDM Thermoplastics Material Overview." [Online]. Available: <http://www.stratasys.com/materials/fdm>. [Accessed: 22-Feb-2017].
- [3] F. Fischer, "THERMOPLASTICS: THE STRONGEST CHOICE FOR 3D PRINTING," *Strat. White Pap.*, 2011.
- [4] "Airbus Standardizes on Stratasys Additive Manufacturing Solutions for A350 XWB Aircraft Supply Chain." [Online]. Available: <http://blog.stratasys.com/2016/10/20/airbus-additive-manufacturing-ultem-9085/>. [Accessed: 22-Feb-2017].
- [5] "ULA to Launch Atlas V Rocket with Stratasys 3D Printed Parts." [Online]. Available: <http://blog.stratasys.com/2015/04/20/atlas-v-rocket-3d-printing/>. [Accessed: 15-Mar-2017].
- [6] F. P. Beer, E. R. Johnston, and J. T. DeWolf, "Stress and Strain - Axial Loading," in *Mechanics of Materials*, 4th ed., New York, NY: McGraw Hill, 2005, p. 57.
- [7] H. Lobo and J. Hurtado, "Characterization and Modeling of Non-Linear Behavior of Plastics." [Online]. Available: [http://www.datapointlabs.com/testpaks/lobo-hurtado/lobo-hurtado\\_paper.html](http://www.datapointlabs.com/testpaks/lobo-hurtado/lobo-hurtado_paper.html). [Accessed: 02-Mar-2017].
- [8] ASTM, "ASTM D638-03: Standard Test Method for Tensile Properties of Plastics," 2004.
- [9] ASTM, "ASTM D3039-2014: Standard Test Method for Tensile Properties of Polymer Matrix Composite Materials," 2014.
- [10] F. Knoop and V. Schoeppner, "Mechanical and Thermal Properties of Fdm Parts Manufactured With

- Polyamide 12," *Solid Free. Fabr. Symp.*, pp. 935–948, 2015.
- [11] a Bagsik, V. Schoeppner, and E. Klemp, "FDM Part Quality Manufactured with Ultem\* 9085," *14th Int. Sci. Conf. Polym. Mater.*, vol. 15, 2010.
- [12] A. Bagsik, V. Schöppner, and K. Paderborn, "Mechanical Properties of Fused Deposition Modeling Parts Manufactured With Ultem\*9085," 2011.
- [13] A. S. El-gizawy, S. Corl, and B. Graybill, "Process-induced Properties of FDM Products," *Int. Conf. Mech. Eng. Technol. Congr. Expo.*, 2011.
- [14] M. Fischer and V. Schöppner, "Fatigue Behavior of FDM Parts Manufactured with Ultem 9085," *Jom*, 2016.
- [15] R. J. Zaldivar, D. B. Witkin, T. McLouth, D. N. Patel, K. Schmitt, and J. P. Nokes, "Influence of processing and orientation print effects on the mechanical and thermal behavior of 3D-Printed ULTEM 9085 Material," *Addit. Manuf.*, vol. 13, pp. 71–80, 2017.
- [16] Stratasys, "ULTEM™ 9085 Datasheet," 2016.
- [17] R. N. Kay, "Effect of Raster Orientation on the Structural Properties of Components Fabricated by Fused Deposition Modeling," p. 165, 2014.
- [18] "ASTM Committee F42 on Additive Manufacturing Technologies." [Online]. Available: <https://www.astm.org/COMMITTEE/F42.htm>. [Accessed: 07-Mar-2017].
- [19] "ASME Committee Pages - Y14 Subcommittee 46 - Product Definition for Additive Manufacturing." [Online]. Available: <https://cstools.asme.org/csconnect/CommitteePages.cfm?Committee=100749850>. [Accessed: 07-Mar-2017].
- [20] "ASTM Additive Manufacturing Technology Standards." [Online]. Available: <https://www.astm.org/Standards/additive-manufacturing-technology-standards.html>. [Accessed: 07-Mar-2017].
- [21] K. P. Motaparti, "Effect of build parameters on mechanical properties of ultem 9085 parts by fused deposition modeling," MISSOURI UNIVERSITY OF SCIENCE AND TECHNOLOGY, 2016.
- [22] X. Liu and V. Shapiro, "Homogenization of material properties in additively manufactured structures," *CAD Comput. Aided Des.*, vol. 78, pp. 71–82, 2016.
- [23] D. Aguilar, S. Christensen, and E. Fox, "3-D Printed Ultem 9085 Testing and Analysis," 2015.
- [24] J. Steuben, "Discrete Element Methods for Additive Manufacturing," 2014. [Online]. Available: <https://steubengineer.wordpress.com/>. [Accessed: 15-Mar-2017].
- [25] "Digimat 2017.1 Delivers the First Simulation Chain for Additive Manufacturing of Polymers." [Online]. Available: <http://www.e-xstream.com/news/digimat-20171-delivers-first-simulation-chain-additive-manufacturing-polymers>. [Accessed: 03-May-2017].
- [26] Dassault Systemes, "Defining Orthotropic Properties," 2016. [Online]. Available: [http://help.solidworks.com/2016/english/solidworks/cworks/r\\_Defining\\_Orthotropic\\_Properties.htm](http://help.solidworks.com/2016/english/solidworks/cworks/r_Defining_Orthotropic_Properties.htm). [Accessed: 15-Mar-2017].
- [27] N. Bakhvalov and G. Panasenko, *Homogenisation: Averaging Processes in Periodic Media*. Kluwer Academic Publishers, 1989.
- [28] 3D Hubs, "Fortus 400mc 3D Printer Reviews & Prices." [Online]. Available: <https://www.3dhubs.com/3d-printers/fortus-400mc>. [Accessed: 15-Mar-2017].
- [29] B. Hudson, "Designing parts for FDM 3D Printing - Overhangs." [Online]. Available: <https://www.3dhubs.com/knowledge-base/designing-parts-fdm-3d-printing#overhangs>. [Accessed: 20-Mar-2017].